Palaeontologia Electronica
http://palaeo-electronica.org

LOCOMOTION IN FOSSIL CARNIVORA: AN APPLICATION OF EIGENSURFACE ANALYSIS FOR MORPHOMETRIC COMPARISON OF 3D SURFACES

P. David Polly and Norman MacLeod

ABSTRACT

We present a new geometric morphometric method called 'eigensurface analysis' for the quantitative analysis of three-dimensional (3D) surfaces. Eigensurface can be viewed as an extension of outline- and landmark-based geometric methods to deal with complete 3D surfaces of objects. We applied eigensurface analysis to the problem of functional inference based on the mammalian calcaneum bone, which is commonly preserved in isolation. Functional interpretations in vertebrate paleontology can be confidently drawn from relatively complete skeletons based on limb proportions and suites of locomotor characters. Interpretations drawn from isolated bones are often less certain, in part because the functionally important features on which the interpretations are based are the curvatures and angles of joint surfaces, which are difficult to quantify using standard linear measurements or 2D geometric morphometric approaches.

Eigensurface analysis allows the entire surface (or surface region) of a specimen to be analyzed by interpolating an evenly spaced grid of semi-landmark points from a standard 3D point-cloud, such as those generated by laser scanners. The same mathematically homologous point grid is fit into each object in a study, which allows the geometry of the grids to be analyzed in the same way one would standard landmark or outline point data. Eigensurface analysis also supports direct shape modelling within the ordination spaces formed to represent shape similarities, thus forming a critical bridge between these mathematical spaces and the qualitative assessment-comparisons of the shapes they represent.

We used the eigensurface method to characterize the calcaneum shape of modern carnivorans in respect to stance, number of digits, and locomotor style. We then quantitatively matched the calcanea of four extinct species to those categories to infer stance, digit number, and locomotor style. Four taxa—*Ictitherium*, an extinct hyaena, *Enhydriodon*, an extinct otter, *Paramachairodus*, an extinct sabre-toothed cat, and *Cynelos*, an extinct amphicyonid—whose anatomy and locomotion are known from independent evidence, were used to assess the effectiveness of eigensurface analysis of individual calcanea. Results allowed us to infer the number of toes, the stance, and the locomotor mode of all four of the taxa correctly. *Cynelos* was incorrectly inferred to have been digitigrade, and *Enhydriodon* was incorrectly inferred to have been terrestrial.

PE Article Number: 11.2.10A

Submission: 4 April 2008. Acceptance: 22 June 2008

Polly, P. David and MacLeod, Norman. 2008. Locomotion in Fossil Carnivora: An Application of Eigensurface Analysis for Morphometric Comparison of 3D Surface. *Palaeontologia Electronica* Vol. 11, Issue 2; 10A:13p;
http://palaeo-electronica.org/2008_2/135/index.html

P. David Polly. Department of Geological Sciences, Indiana University, 1001 E. 10th Street
Bloomington, IN 47401 USA, pdpolly@indiana.edu
Norman MacLeod, Department of Palaeontology, The Natural History Museum, Cromwell Road
London SW7 5BD United Kingdom, nm@nhm.ac.uk

KEYWORDS: Carnivora, Eigensurface, Geometric Morphometrics

INTRODUCTION

Three dimensional (3D) surface scans of complicated morphological structures (e.g., bones, teeth and shells) are increasingly easy to generate. Laser scanning, pin scanning, computerized tomography, *X*-ray microtomography, and magnetic resonance imaging all produce 3D data representing the surfaces of modern and fossil specimens (e.g., Jernvall and Selänne 1999; Ungar and Williamson 2000; Lyons et al. 2000; Sutton et al. 2001; Wilhite 2003; Polcyn et al. 2002, 2005; Alonso et al. 2004; Colbert 2005; Polly et al. 2006; Schwarz et al. 2005; Evans et al. 2007; Evans and Fortelius 2007). From such data it is possible to calculate volumes, surface areas, and morphological indices that can be used to describe functional or taxonomic properties.

The ready availability of 3D scan data make desirable the quantitative comparison and analysis of 3D surface shapes themselves. Here we present an approach for the direct morphometric analysis of 3D surfaces. Our method, which we have called 'eigensurface analysis' (see also MacLeod 2008; Polly 2008), is related to geometric morphometric techniques such as the analysis of landmarks (Bookstein 1991; Rohlf 1993; Dryden and Mardia 1998; Zelditch et al. 2004) and eigenshape analysis of outlines (Lohmann 1983; MacLeod and Rose 1993; MacLeod 1999). Our method reduces the original 3D scan of surface points to a grid of quasi-evenly spaced points. We discuss several approaches to choosing the point grid, but here we use a small number of landmark points on the specimen to superimpose the point cloud-represented surfaces before interpolating the grid of eigensurface points. Principal components of the covariance matrix of the grid points are then used to define the major and minor vectors of the shape variation, which are then used as the axes of a coordinate system to form shape spaces in which similarities and differences between the surface shapes can be portrayed. The coordinate positions of the surfaces projected into these shape spaces can also be used for further statistical analysis.

To illustrate use of the eigensurface technique, we perform an example analysis to infer locomotor morphology from the calcanea of four extinct mammalian carnivorans. The calcaneum is the largest bone in the mammalian ankle. With the distal tibia, it forms the primary ankle joint, and its long posterior tubercle acts as the lever arm for plantarflexion of the foot, powered by the gastrocnemius and soleus muscles that attach to its end via the Achilles tendon (Figure 1). The form of the calcaneum is closely related to locomotor function. However, because the functional aspects are subtle, 3D configurations of articular facets and bony processes are difficult to capture in a quantitative analysis. We applied eigensurface analysis to the calcanea of living carnivorans with diverse locomotor habits to extract quantitatively those aspects of the form that are associated with locomotor categories and use that information to categorize the extinct taxa. A detailed analysis of the locomotor morphology of the living taxa using an earlier version of eigensurface is presented elsewhere (Polly 2008). Here we concentrate on the fossil taxa and focus on a description of the morphometric method.

Our goal was to test the ability of eigensurface to assign calcanea to locomotor categories. We chose four fossil species whose locomotor specializations are understood based on other skeletal and palaeoenvironmental evidence (Figure 2). Three of the species are from the classic Miocene site of Pikermi, Greece (Black et al. 1980; Solounias 1981). *Paramachairodus orientalis* was a cat somewhat larger than the modern Leopard. Like other felids, *P. orientalis* had four hind toes and walked with a digitigrade stance (Pilgrim 1931). *Paramachairodus* had smaller, more flexible hindlimbs than the Leopard and was probably a better climber (Turner 1997). *Enhydriodon latipes* was a large otter. Like living otters, it had five hind toes and a flexible ankle used for both walking and swimming (Pilgrim 1931). *Ictitherium viverrinum*

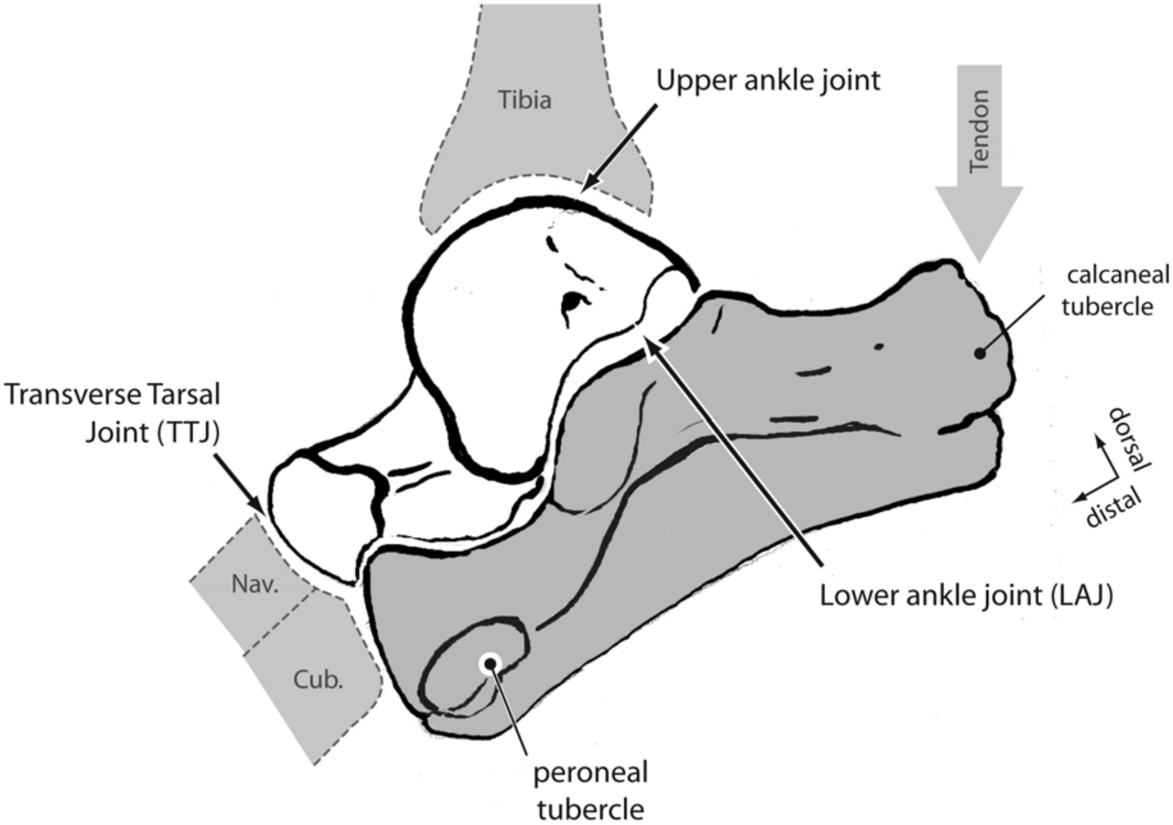

Figure 1. Anatomy and function of the mammalian calcaneum. The calcaneum is shown in life position in lateral view (grey) along with the astragalus (white). The relation of these two bones to the distal tibia, navicular (nav.), and cuboid (cub.) bones are also indicated. The main upper ankle joint is between the tibia and astragalus, but there is also a joint between the astragalus and calcaneum (lower ankle joint) and between those two bones and the navicular and cuboid, respectively (transverse tarsal joint). Extension of the foot is powered by contraction of the Achilles tendon (arrow) pulling dorsally on the calcaneal tubercle.

was a medium-sized carnivoran related to modern hyaenas and like them had four hind toes and a digitigrade, terrestrial stance (Pilgrim 1931; Werdelin 1988). The fourth species is an amphicyonid from the Oligocene of Allier, France, *Cynelos lemanensis*. This “bear dog” species was a five toed plantigrade omnivore.

MATERIALS AND METHODS

Bones

The dorsal side of the calcaneum of 10 living species of Carnivora were scanned in three dimensions (see below, Table 1). These same scans were used in a previous study on the evolution of locomotor morphology in living Carnivora (Polly 2008).

Each bone was assigned one of the following locomotor types following Van Valkenburgh (1985) and Taylor (1976). **Terrestrial:** animals that spend most of their time on the ground (e.g.*,* dogs and hyenas). **Scansorial**: animals that spend considerable time on the ground, but are also good climbers (e.g.*,* most felids). **Arboreal:** animals that spend most of their time in trees (e.g., olingos, red pandas). **Natatorial**: animals that spend time in both the water and on land (e.g.*,* otters).

Stance, or the position of the heel during normal locomotion (Clevedon Brown and Yalden 1973; Gambaryan 1974; Hildebrand 1980), was recorded for each species using the following categories. **Plantigrade**: animals that walk with their heels touching the ground (e.g., red pandas). **Semidigitigrade:** animals that often keep their heels elevated during locomotion (e.g., many mustelids). **Digitigrade:** animals always have their heels elevated during normal locomotion, using the metatarsus as an additional limb segment (e.g.,

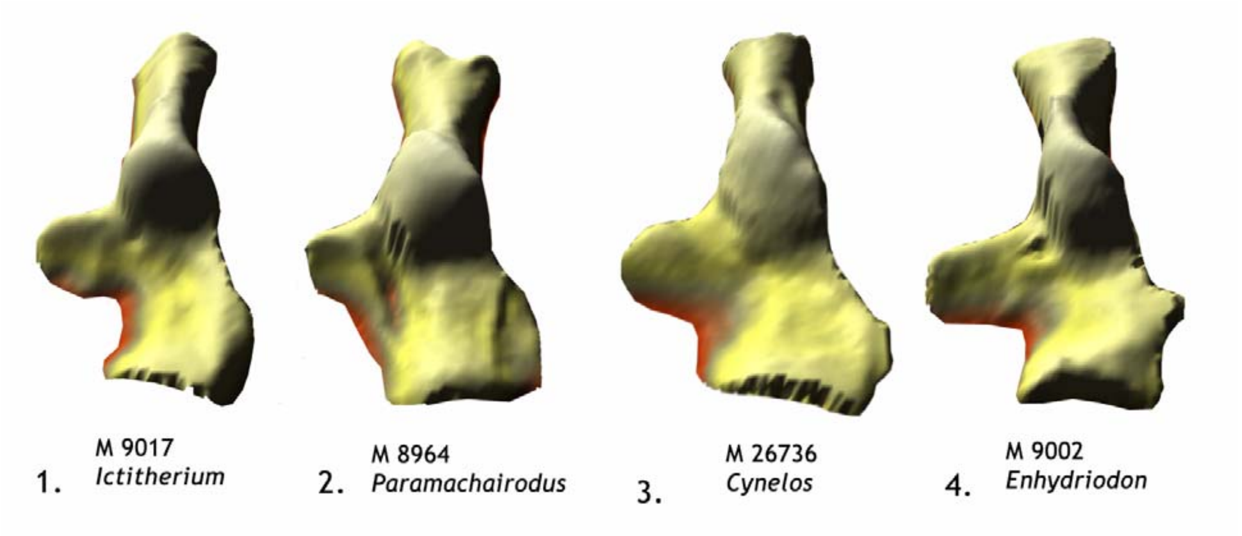

Figure 2. Dorsal calcaneum of: **2.1** *Ictitherium viverrinum*, a hyaenid; **2.2** *Paramachairodus orientalis*, a felid; **2.3** *Cynelos lemanensis*, an amphicyonid; and **2.4** *Enhydriodon latipes*, an otter. The figures are surface renderings made from 3D point clouds. The crinkled edges visible around the margins are artefacts of the renderings, not the scan data that were used in the analysis.

dogs, felids). The number of toes on the hind foot was also recorded as four or five.

Four fossil calcanea were also scanned in dorsal view (Table 2). These taxa were characterized with the same categories using the same criteria as the living taxa (b). These characterizations were used to assess the accuracy with which eigensurface could be used to assign characterizations using the modern calcanea (see below).

Scans

Calcanea from the living species were scanned at Queen Mary, University of London, in 2005 using a Roland Picza Pix-4 3D pin scanner. This scanner drops a pin onto the surface of the bone and records the three-dimensional *x,y,z* coordinates of that surface point. The scanner moves across the surface of the object dropping the pin in a grid pattern. Scans of the fossil calcanea were made at The Natural History Museum, London, in

Table 1. Modern carnivoran species used in this study with associated data.

Species	Common Name	Family	Stance	Digits	Locomotor Mode
Ailurus fulgens	Red panda	Ailuridae	Plantigrade	5	Arboreal
Bassaricyon gabbii	Bushy-tailed olingo	Procyonidae	Plantigrade	5	Arboreal
Canis familiaris	Dog (Greyhound)	Canidae	Digitigrade	4	Terrestrial
Crocuta crocuta	Spotted hyaena	Hyaenidae	Digitigrade	4	Terrestrial
Felis catus	Domestic cat	Felidae	Digitigrade	4	Scansorial
Leptailurus serval	Serval	Felidae	Digitigrade	4	Terrestrial
Lutra lutra	European otter	Mustelidae	Semidigitigrade	5	Natatorial
Lynx rufus	Bobcat	Felidae	Digitigrade	4	Scansorial
Meles meles	Badger	Mustelidae	Semidigitigrade	5	Semifossorial
Mustela putorius	Polecat	Mustelidae	Semidigitigrade	5	Terrestrial

Table 2. The four fossil species of the mammalian order Carnivora assessed in this study. All material is housed in the Palaeontology Department of London's Museum of Natural History.

Species	Family	Locality	Age	Specimen number	Stance	Digits	Locomotor Mode
Cynelos lemanensis	Amphicyonidae	Allier, France (unspecified)	Early Miocene / Late Oligocene	M 26736	Plantigrade	5	Terrestrial
Enhydriodon latipes	Mustelidae	Pikermi, Greece	Miocene (MN 12)	M 9002	Semidigitigrade	5	Natatorial
Ictitherium viverrinum	Hyaenidae	Pikermi, Greece	Miocene (MN 12)	M 9107	Digitigrade	4	Terrestrial
Paramachairodus orientalis	Felidae	Pikermi, Greece	Miocene (MN 12)	M 8964	Semidigitigrade	4	Terrestrial

2006 using a Konica-Minolta VIVID 910 laser scanner. This scanner uses reflections of laser-beam light to determine the distance between the surface of a specimen and the scanner. By scanning the laser beam across the field of view, a 3D map of the specimen's surfaces is recorded as a set of *x,y,z* coordinate points. This point cloud can then be operated on using specialized 3D imaging software (e.g., used to construct a virtual facsimile of the specimen, interpolated to optimize representation of the surface, edited to fill holes or eliminate scanning artefacts, resampled to reduce redundancy). All scans were exported as ASCII *x,y,z* point clouds using the commercial software bundled with the respective scanners.

Eigensurface Analysis

Eigensurface is the analysis of a standardized set of *x,y,z* coordinate points representing the nodes of a grid. These points represent an interpolated subsample of the point cloud of points from a three-dimensional scan of an object's surface. First the *x,y,z* coordinate datasets representing the processed object scans were rotated to a topologically 'homologous' orientation and then a gridding algorithm was applied. All scans were translated, scaled, and aligned using Procrustes (GLS) superimposition (Rohlf 1990) based on five landmark points taken from among those represented by the scan surface (Figure 3.1). The Procrustes fit was optimized using only the five landmarks, but the entire surface scan was carried with those points as they were superimposed on the sample mean

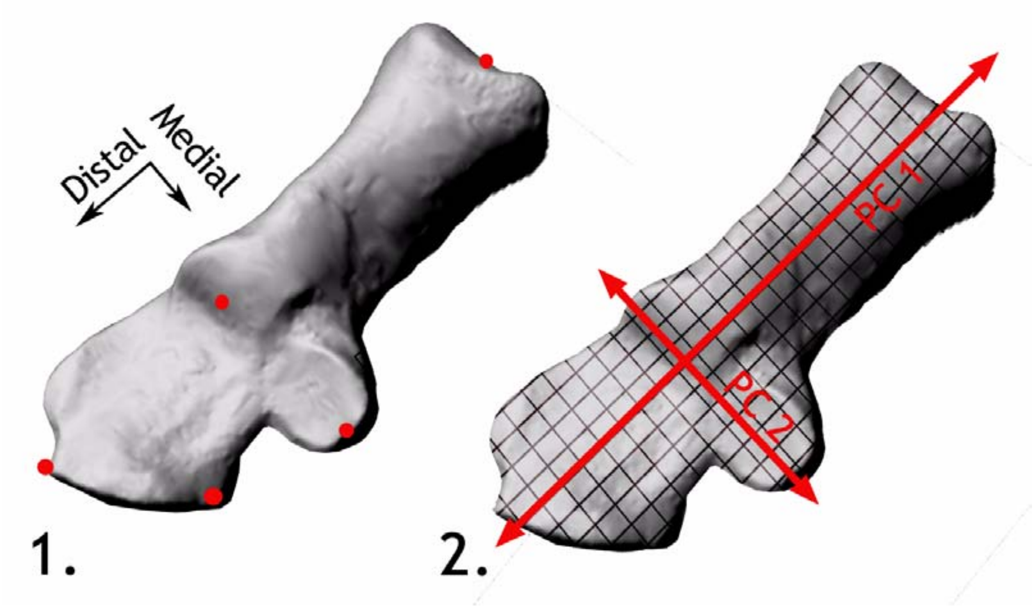

Figure 3. 3.1 Five landmarks used to superimpose the surface scan data prior to fitting the analytical surface points. **3.2** Schematic diagram of the grid laid onto each surface to divide it into subequally spaced analytical points.

shape. This operation transforms the raw *x,y,z* coordinates by removing differences in size, position, and rotation. The procedure for orienting the scan data was nearly identical to the one described by Wiley et al. (2005), but those authors used the scan data for illustrative purposes rather than further analysis.

Next an analytical surface grid was extracted from the Procrustes-oriented points. This grid was created by 'sectioning' each scan along its first principal component (the major axis of the object) into a fixed number of rows (Figure 3.2). Each row was then divided along the second principal component to create square sections, each of which contains one or more surface points (the exact number will depend on the scanning density and the number of sections). This procedure was repeated for each of the scans. Depending on the shape of the original object, the same row may have more sections on one object than on another. A standardized number of sections was determined by taking the sample median number in each row for the entire sample of objects. (See MacLeod 2008 for an alternative eigensurface gridding procedure.) The standardized sections were then applied to all the specimens. The analytical surface grids were then created by placing one 3D point in each section using the median *x,y,z* coordinate of the original scan points in that section. For the fossil carnivore analysis each calcaneum was gridded into 50 rows along the first principal component, which yielded a total of 2,190 nodal grid points.

All points in the analytical surface grids were then superimposed using the Procrustes (GLS) method to remove any residual differences in size, translation, and rotation. The rest of the procedure is identical to standard methods for comparing geometric landmark points (e.g., Rohlf 1993; Dryden and Mardia 1998; interested readers should refer to these works for equations and algorithms to carry out the following steps). The mean surface shape, or consensus, was subtracted from the Procrustes superimposed data to produce Procrustes residuals. A principal components analysis (PCA) was carried out on the covariance matrix of these residuals to decompose this shape similarity matrix into its respective eigenvalues and eigenvectors. We used singular value decomposition (SVD) to calculate the PC eigenvalues and eigenvectors because standard eigen-decomposition algorithms cannot be used on matrices of reduced rank, which result from the loss of dimensionality through Procrustes superimposition. To make the computation less intensive, a 'Q-mode' covariance matrix of the objects was calculated from the transpose of the Procrustes residuals to produce matrices of object eigenvectors and eigenvalues, **U** and **V**, respectively. Eigenvectors for the variables were calculated as **U.R**, where **R** is the matrix of Procrustes residuals. Principal component scores for the objects were calculated by scaling the transpose of **U** by the square root of **V**. The PC object scores were used as shape coordinates for subsequent analysis, and the eigenvectors for the variables defined the coordinate system for the shape space. PC scores were used as shape coordinates because their number is equal to the real degrees of freedom in the data set and because each PC is mathematically orthogonal (there is no correlation between scores on one PC and another), which simplifies statistical analysis (Rohlf 1993; Dryden and Mardia 1998).

Three-dimensional shape models were constructed for the first three PCs to illustrate the shape variation described by each. Models were constructed using the standard geometric morphometric procedure of multiplying the point in shape space to be modelled by the eigenvector associated with that PC and adding the result to the mean shape (Rohlf 1993). The same procedure was used for 2D eigenshape results (see MacLeod (1999) and 3D eigensurface results (see Polly 2008).

The PC score shape coordinates are quantitative representations of the variance in shape of the calcaneum surface; collectively the variance in the PC scores and the Euclidean distances between specimens in PC space preserve the original variance and distances between the gridded scans. All PC axes were retained for evaluating shape similarity. All transformations were performed in Mathematica 5.0©.

Functional Analysis

The average calcaneum shape was calculated for each locomotor mode, stance type, and digit number using only the scores of the living species. The fossil calcanea were categorized in each of these three categories by finding which of the averages it was closest to. Closeness of fit was measured as the Procrustes distance, which is the square root of the sum-of-squared distances between the superimposed landmarks or between the vectors of PC scores for two objects and is a Euclidean measure of distance similar to those used in many cluster analyses.

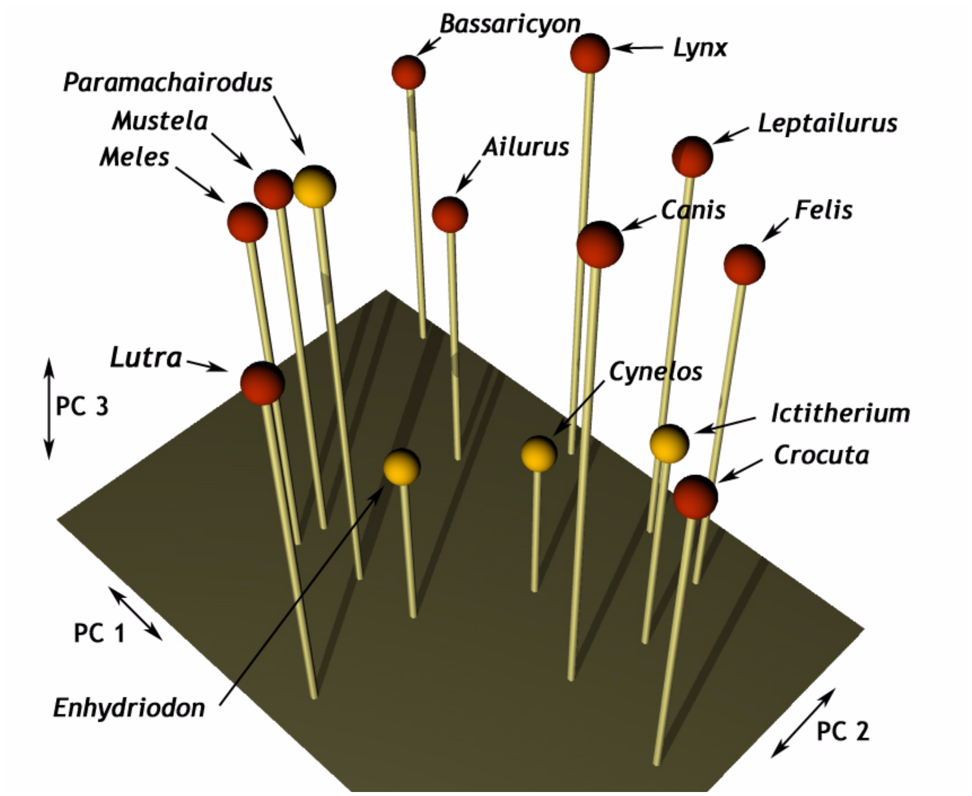

Figure 4. Scatter of the calcaneal shapes in the first three dimensions of the principal components shape space. Extant taxa are represented by red balls, fossil taxa by yellow balls.

RESULTS AND DISCUSSION

Principal Components

A principal components scatter of the fossil and recent calcanea is shown in Figure 4. The distribution of shapes was primarily functional, though low-level taxonomic relationships were also apparent in that the felids and mustelids each formed clusters. Higher level phylogenetic relationships were not reflected in the shape space distributions. *Canis*, for example, fell close to the felids, even though it is only distantly related, whereas *Crocuta* fell far from its kin the felids.

The first principal component, which explained 28.7% of the total variance in shape (Table 3), described differences in calcaneum shape associated with mobility at the lower ankle joint (LAJ) and stance. Plantigrade taxa with mobile LAJs like *Bassaricyon* and *Ailurus* fell at one end of PC 1 and digitigrade taxa with immobile LAJs like *Crocuta*, *Felis*, and *Canis* were at the opposite end. Calcanea with broad sustentacular facets positioned anterior to the calcaneoastragalar facet and broad distal regions with peroneal tubercle were found at the mobile end of the axis, whereas calcanea with proportionally smaller sustentacular facets positioned lateral to the calcaneoastragalar facet and a narrow, angled distal calcaneum were at its immobile end (Figure 5.1).

PC 2 explained 18.5% of the total variance (Table 3) and also described functional differences of the calcaneum. Calcanea with blocky distal ends, gently curved calcaneoastragalar facets, and thick calcaneal processes were at one end of the axis and bones with longer distal ends, sharply curved calcaneoastragalar facets, and narrow calcaneal processes were at the opposite end. These morphologies are associated with plantigrade and digitigrade postures, respectively.

PC 3 explained 13.9% of the total variance (Table 3). Overall breadth relative to length of the calcaneum was described by this axis, include correlation of the length of the sustentacular and peroneal processes. The mediolateral curvature of the calcaneoastragalar facet was also associated with this axis.

Locomotor Differences in Extant Taxa

Carnivores with four toes had, on average, narrower distal calcanea and broader sustentacu-

Table 3. Eigenvalues and percent variances explained for the PCA.

	Eigenvalue	% Variance Explained	Cumulative % Variance Explained
PC 1	1.38E-05	0.29	0.29
PC 2	8.89E-06	0.18	0.47
PC 3	6.68E-06	0.14	0.61
PC 4	4.09E-06	0.09	0.70
PC 5	3.70E-06	0.08	0.77
PC 6	2.31E-06	0.05	0.82
PC 7	2.11E-06	0.04	0.87
PC 8	1.72E-06	0.04	0.90
PC 9	1.46E-06	0.03	0.93
PC 10	1.19E-06	0.02	0.96
PC 11	9.89E-07	0.02	0.98
PC 12	5.75E-07	0.01	0.99
PC 13	5.38E-07	0.01	1.00

lar facets than did those with five toes (Figure 6.1). Plantigrade taxa had broader sustentacular facets placed more distally than did digitigrade taxa (Figure 6.2). The shape of the arboreal calcaneum was similar to the plantigrade one, and the average terrestrial calcaneum was similar to the digitigrade one (Figure 6.3). Scansorial and natatorial calanea both have distal ends that are angled medially on average, with a larger peroneal process on the natatorial one. Semifossorial calcanea have a straight distal end, but a large peroneal process. Additional functional differences have been discussed in Polly (2008).

Locomotor Inference in Fossil Taxa

The four fossil calcanea were categorized for digit number, stance, and locomotor type by finding the closest match between their shape and the

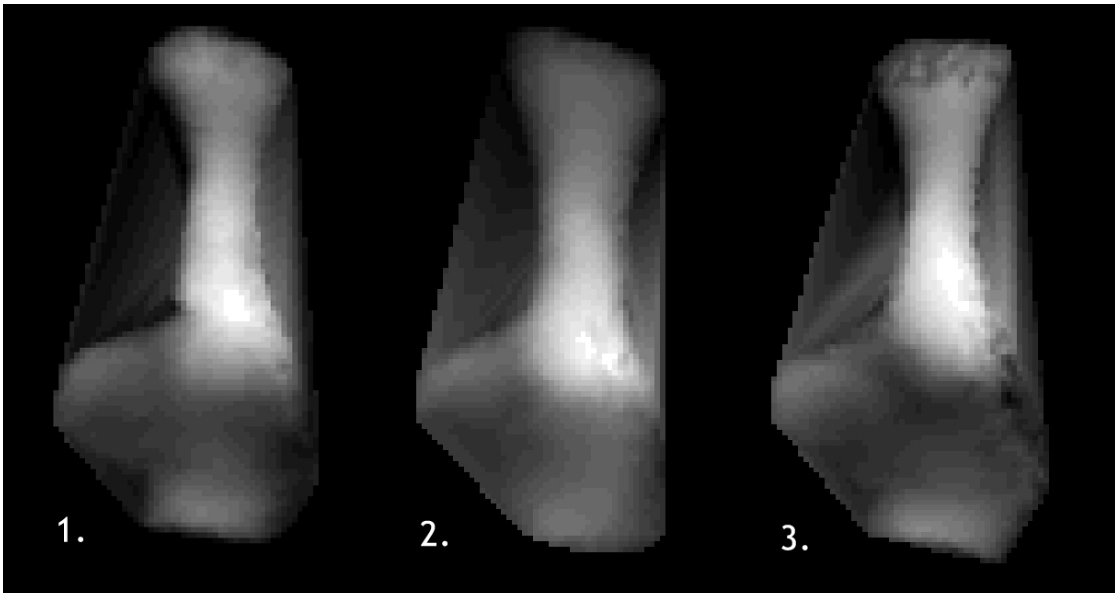

Figure 5. Animated models of the shape variation described by the first three principal components. **5.1**. Principal component 1. **5.2.** Principal component 2. **5.3.** Principal component 3. These models are mathematical representations of the shape variation on each respective PC based on the eigenvector loadings.

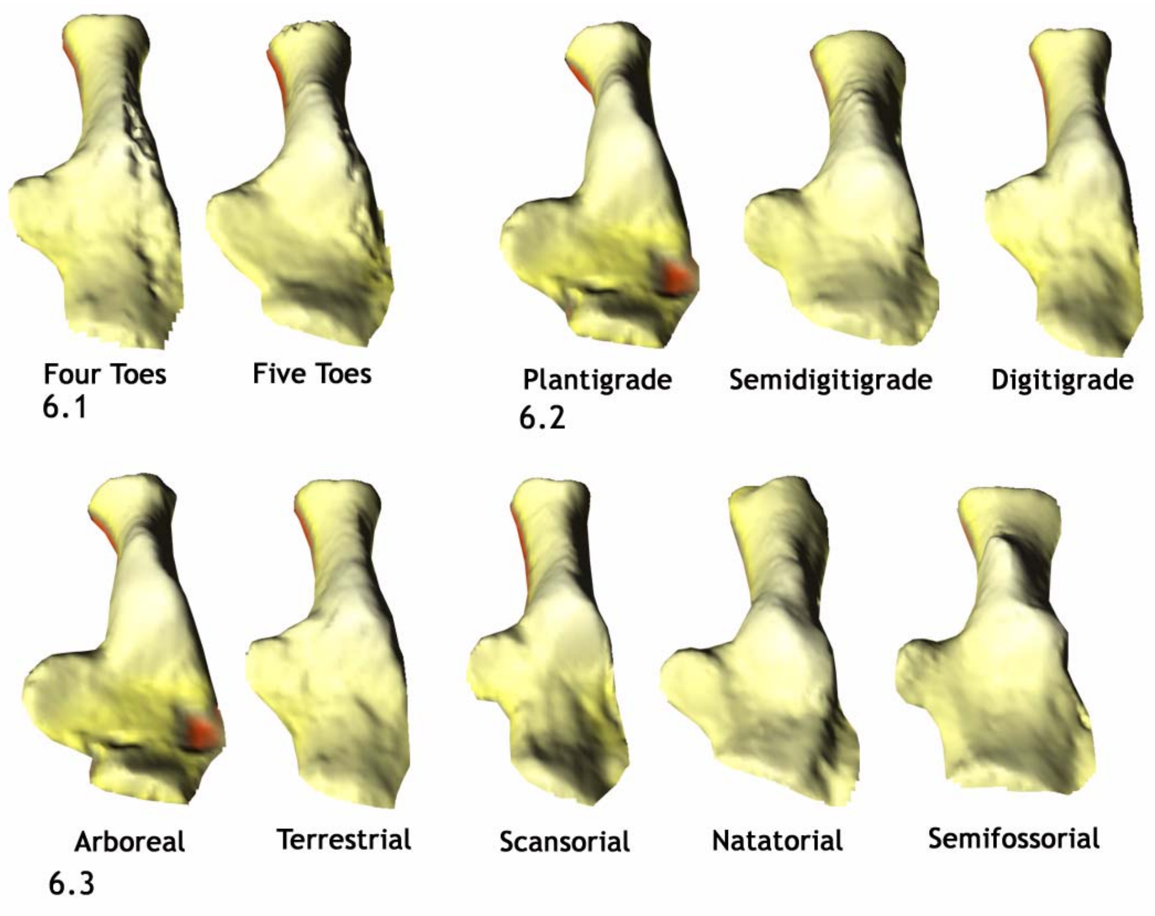

Figure 6. Mean calcaneal surface shapes based on the sample of extant taxa. **6.1.** Mean shape of four and five toed taxa. **6.2.** Mean shape of plantigrade, semidigitigrade, and digitigrade taxa. **6.3.** Mean shape of arboreal, terrestrial, scansorial, natatorial, and semifossorial taxa.

shapes shown in Figure 6 (Table 4). In total 12 categorizations were made, three for each of the four taxa. Of those, 10 were correct and two were incorrect (Table 5). The amphicyonid *Cynelos* was incorrectly categorized as being digitigrade when it was likely plantigrade or semidigitigrade, and the otter *Enhydriodon* was categorized as terrestrial when it was really natatorial. *Cynelos* was probably miscategorized because it has a more posteriorly positioned sustentacular facet than does the plantigrade average. The fit of *Cynelos* to the digitigrade category was only marginally better than to the semidigitigrade one (Procrustes distances 0.0083 and 0.0098, respectively). *Enhydriodon* was probably miscategorized because the distal end of the calcaneum is not as angled, and the peroneal process is not as large as in the modern otter.

Cluster analysis (the grouping of specimens based on a measure of distance, often a Euclidean distance like the Procrustes distance) and Discriminant Function Analysis (DFA) could be used in place of our Procrustes matching and probability calculation. We preferred to match each unknown specimen to the mean shapes in each category, which is basically finding the fossil's nearest neighbour in multivariate shape space, because clustering algorithms necessarily distort shape distances as a compromise in creating a tree topology (Sneath and Sokal 1973; Prager and Wilson 1978). The probability that all but two categorizations could have been correct by chance is real, but small. The probability that toe number could have been categorized correctly in all four taxa equals the probability of a correct assignment (50%) multiplied over the number of assignments made (4): $0.5^4 = 0.0625$. The probability that stance could have been categorized correctly in three taxa and wrongly in one is the probability of a correct assignment (33.3%) multiplied over the number of correct assignments (3) multiplied by the probability of one incorrect assignment (66.7%): $0.33^3 * 0.67 =$

Table 4. Procrustes fits of four fossil calcanea to modern locomotor data. Result were obtained by calculating the Procrustes distance between the fossil and the average types shown in **Figure 6**.

	Number of Toes		**Stance**			**Locomotor Type**				
	Four	**Five**	**Plantigrade**	**Digitigrade**	**Semidigitigrade**	**Arboreal**	**Terrestrial**	**Scansorial**	**Natatorial**	**Semifossorial**
Cynelos lemanensis	0.0079	0.0069	0.0101	0.0083	0.0094	0.0101	0.0083	0.0087	0.0100	0.0098
Enhydriodon latipes	0.0091	0.0087	0.0112	0.0100	0.0095	0.0111	0.0093	0.0108	0.0108	0.0097
Ictitherium viverrinum	0.0067	0.0076	0.0107	0.0067	0.0104	0.0107	0.0070	0.0076	0.0112	0.0112
Paramachairodus orientalis	0.0088	0.0092	0.0122	0.0087	0.0103	0.0122	0.0083	0.0100	0.0107	0.0113

Table 5. Results of automated locomotor analysis of four fossil calcanea.

Species	**Toes**	**Correct?**	**Stance**	**Correct?**	**Locomotor Type**	**Correct?**
Cynelos lemanensis	5	Yes	Digitigrade	No	Terrestrial	Yes
Enhydriodon latipes	5	Yes	Semidigitigrade	Yes	Terrestrial	No
Ictitherium viverrinum	4	Yes	Digitigrade	Yes	Terrestrial	Yes
Paramachairodus orientalis	4	Yes	Semidigitigrade	Yes	Terrestrial	Yes

0.025. And the probability that locomotor mode could have been categorized correctly in three taxa and wrong in one is the probability of a correct assignment (20%) multiplied over the number of correct assignments (3) multiplied by the probability of one incorrect assignment (80%): $0.2^3 * 0.8 = 0.0064$. The probability of obtaining only two incorrect results across the whole analysis is obtained by multiplying these three probabilities together: $P = 0.0625 * 0.025 * 0.0064 = 9.8 \text{ x } 10^{-6}$.

The Eigensurface Method

The gridding algorithm used here is an improvement over the one described by Polly (2008), who fit a rectangular grid of points to the surface. The present algorithm produces analytical points that are spread more evenly across the surface than the earlier algorithm. The density of points across the surface determines how much each part of the morphology contributes to the analysis; high densities of points on particular parts cause those parts to be weighted more heavily in the analytical results. This approach differs, however, from that used by MacLeod (2008) to analyze bivalve shell shape using an algorithm to reduce ‘edge effects,’ and is especially useful when applying coarse grids to specimen surfaces.

The approach used here also differs from that used by Mitteröcker et al. (2005), who extended the use of sliding semi-landmarks to 3D surfaces of human skulls. Their approach used a skeleton of curves to represent the main 3D contours of an object. The curves were then fitted with sliding semi-landmarks positioned so as to minimize differences in shape among the objects (Bookstein 1997). The semi-landmark approach uses a much lower density of surface points than does ours, and so captures the general configuration of the object without capturing finer-scale details of the surface variation. Advantages of the semi-landmark approach compared to ours is that the semi-landmark method can be applied to topographically complicated structures (e.g., mammalian skulls); disadvantages compared to ours is that the semi-landmark method suffers even more greatly from variable densities of points, thus weighting some regions of the object more because regions with high point density contribute more variance to the overall shape than do those with lower point density.

Wiley et al. (2005) described a procedure for “evolutionary morphing” of primate skulls, which is similar to Mitteröcker et al.’s (2005) method in that it uses semi-landmarks to represent large patches of surface, but also used individual landmark points to represent parts of morphology that could easily be characterized that way. Wiley et al.’s analysis was carried out on the landmark and semi-landmark points, which were then used to “morph” entire scan data sets.

Three-dimensional surface shape has also been analyzed using spherical Fourier harmonic descriptors (SPHARM) of surface scan data (Styner et al. 2006; McPeek et al. 2008). Whereas the method of deriving shape coordinates from the *x,y,z* surface data is very different with Fourier harmonics, the subsequent methods for statistical analysis and shape visualization are similar to our method and the ones of Mitteröcker et al. (2005) and Wiley et al. (2005).

CONCLUSIONS

That the shape of the carnivoran calcaneum is related to locomotor function comes as no surprise. The mammalian ankle joint is well-studied and the relation of form and function well-understood (Jenkins and McClearn 1984; Szalay 1977, 1994; Taylor 1970, 1976, 1988, 1989). But quantitative functional analysis of tarsal bones has not been as successful as it has with limb proportions or humerus, ulna, or radius shape (e.g., Andersson 2004; Andersson and Werdelin 2003; MacLeod and Rose 1993; Van Valkenburgh 1985) because the functional features of tarsals are the curved surfaces of their interlocking joints.

The success of our 3D eigensurface method, while qualified, is encouraging. Eigensurface analysis of the 3D topography of calcanea sorted them into the same functional spectrum that qualitative functional analysis would have. Importantly, the quantitative descriptors of calcaneum shape allowed fossil calcanea to be assigned to the functional categories of stance, digit number, and locomotor style nearly as accurately as was possible through qualitative functional analysis of the entire postcrania. The general agreement of our quantitative results with previous qualitative assessments of locomotor function in four extinct carnivorans suggests that isolated calcanea, which are comparatively common in the mammalian fossil record, could be interpreted functionally with nearly the same degree of confidence as we now place in interpretations based on complete limbs.

ACKNOWLEDGEMENTS

A. Currant and J. Hooker provided access to and help with both recent and fossil tarsals in the collections of the Department of Palaeontology, The Natural History Museum, London. L. Werdelin provided information on the locomotor morphology of *Ictitherium*.

REFERENCES

Alonso, P.D., Milner, A.C., Ketcham, R.A., Cookson, M.J., and Rowe, T.B. 2004. The avian nature of the brain and inner ear of Archaeopteryx. *Nature*, 430:666-669.

Andersson, K. 2004. Elbow-joint morphology as a guide to forearm function and foraging behaviour in mammalian carnivores. *Zoological Journal of the Linnean Society*, 142:91-104.

Andersson, K. and Werdelin, L. 2003. The evolution of cursorial carnivores in the Tertiary: implications of elbow-joint morphology. *Proceedings of the Royal Society of London B*, 270:S163-S165.

Black, C.C., Krishtalka, L., and Solounias, N. 1980. Mammalian fossils of Samos and Pikermi. Part 1. The Turolian rodents and insectivores of Samos. *Annals of Carnegie Museum,* 49:359-378.

Bookstein, F.L. 1991. Morphometric tools for landmark data: geometry and biology. Cambridge University Press, Cambridge.

Bookstein, F.L. 1997. Landmark methods for forms without landmarks: morphometrics of group differences in outline shape. *Medical Image Analysis*, 1:225-243.

Clevedon Brown, J., and Yalden, D.W. 1973. The description of mammals -2. Limbs and locomotion of terrestrial mammals. *Mammal Review*, 3:107-135.

Colbert, M.W. 2005. The Facial Skeleton of the Early Oligocene *Colodon* (Perissodactyla, Tapiroidea), *Palaeontologia Electronica* 8.1.2A:27p, 600KB; http://palaeo-electronica.org/paleo/2005_1/colbert12/issue1_05.htm

Dryden, I.L., and Mardia, K.V. 1998 *Statistical Analysis of Shape*. John Wiley & Sons.

Evans, A.R., and Fortelius, M. 2007. Three-dimensional reconstruction of tooth relationships during carnivoran chewing. *Palaeontologia Electronica*, 11.2.10A.

Evans, A.R., Wilson, G.P., Fortelius, M., and Jernvall, J. 2007. High-level similarity of dentitions in carnivorans and rodents. *Nature*, 445:78-81.

Gambaryan, P.P. 1974. How Mammals Run: Anatomical Adaptations. New York: John Wiley and Sons.

Hildebrand, M. 1980. The adaptive significance of tetrapod gait selection. *American Zoologist*, 20:255-267.

Jenkins, F.A., and McClearn, D. 1984. Mechanisms of hind foot reversal in climbing mammals. *Journal of Morphology,* 182:197-219.

Jernvall, J., and Selänne, L. 1999. Laser Confocal Microscopy and Geographic Information Systems in the Study of Dental Morphology. *Palaeontologia Electronica*, 2.1.18, 905KB. http://palaeo-electronica.org/1999_1/confocal/issue1_99.htm

Lohmann, G.P. 1983. Eigenshape analysis of microfossils: A general morphometric method for describing changes in shape. *Mathematical Geology*, 15:659-672.

Lyons, P.D., Rioux, M., and Patterson, R.T. 2000. Application of a Three-Dimensional Color Laser Scanner to Paleontology: an Interactive Model of a Juvenile *Tylosaurus* sp. Basisphenoid-Basioccipital. *Palaeontologia Electronica,* 3.2.5:16 pp., 2.04MB. http://palaeo-electronica.org/2000_2/mosasaur/issue2_00.htm

MacLeod, N. 1999. Generalizing and extending the eigenshape method of shape space visualization and analysis. *Paleobiology,* 25:107-138.

MacLeod, N. 2008. Understanding morphology in systematic contexts: 3D specimen ordination and 3D specimen recognition. Pp. 143–210. In Q. Wheeler (ed.), The New Taxonomy. CRC Press, Taylor & Francis Group, London.

MacLeod, N., and Rose, K.D. 1993. Inferring locomotor behavior in Paleogene mammals via eigenshape analysis. *American Journal of Science*, 293-A:300-355.

McPeek, M.P., Shen, L., Torrey, J.Z., and Farid, H. 2008. The tempo and mode of 3-dimensional morphological evolution in male reproductive structures. *American Naturalist*, 171: E158-E178.

Mitteröcker, P., Gunz, P., and Bookstein, F.L. 2005. Heterochrony and geometric morphometrics: a comparison of cranial growth in *Pan paniscus* versus *Pan troglodytes*. *Evolution and Development*, 7:244-258.

Pilgrim, G.E. 1931. Catalogue of the Pontian Carnivora of Europe in the Department of Geology, British Museum (Natural History). British Museum (Natural History): London.

Polcyn, M.J., Jacobs, L.L., and Haber, A. 2005. A morphological model and CT assessment of the skull of *Pachyrachis problematicus* (Squamata, Serpentes), a 98 million year old snake with legs from the Middle East. *Palaeontologia Electronica*, 8.1.26A.

Polcyn, M.J., Rogers, J.V. II, Kobayashi, Y., and Jacobs, L.L. 2002. Computed Tomography of an Anolis Lizard in Dominican Amber: Systematic, Taphonomic, Biogeoraphic, and Evolutionary Implications. *Palaeontologia Electronica,* 5.1.1:13 pp., 5.6MB. http://www-odp.tamu.edu/paleo/2002_1/amber/issue1_02.htm

Polly, P.D. 2008. Adaptive Zones and the Pinniped Ankle: A 3D Quantitative Analysis of Carnivoran Tarsal Evolution. Pp. 165-194. In Sargis, E. and Dagosto, M. (eds.), *Mammalian Evolutionary Morphology: A Tribute to Frederick S. Szalay.* Springer: Dordrecht, The Netherlands.

Polly, P.D., Wesley-Hunt, G.D., Heinrich, R.E., Davis, G., and Houde, P. 2006. Earliest known carnivoran auditory bulla and support for a recent origin of crown-group Carnivora (Eutheria, Mammalia). *Palaeontology*, 49:1019-1027.

Prager, E.M., and Wilson, A.C. 1978. Construction of phylogenetic trees for proteins and nucleic acids: empirical evaluations of alternative matrix methods. *Journal of Molecular Evolution*, 11:129-142.

Rohlf, F.J. 1990. Rotational fit Procrustes methods. In Rohlf, F.J., and Bookstein, F.L. (eds.), Proceedings of the Michigan Morphometrics Workshop. *University of Michigan Museum of Zoolology Special Publication*, 2:227-236.

Rohlf, F.J. 1993. Relative warp analysis and an example of its application to mosquito wings. Pp. 131-159. In Marcus et al. (eds.), Contributions to morphometrics. Musuo Nacionale de Ciencias Naturales.

Schwarz, D., Meyer, C., Lehmann, E., Vontobel, P., and Bongartz, G. 2005. Neutron tomography of internal structures of vertebrate remains: a comparison with X-ray computed tomography. *Palaeontologia Electronica*, 8.2.30A.

Solounias, N. 1981. Mammalian fossils of Samos and Pikermi. Part 2. Resurrection of a classic Turolian fauna. *Annals of Carnegie Museum*, 50:231-270.

Sneath, P.H.A., and Sokal, R.R. 1973. *Numerical Taxonomy*. W.H. Freeman and Co., San Francisco.

Styner, M., Oguz, I., Xu, S., Brechbuehler, C., Pantazis, D., Levitt, J.J., Shenton, M.E., and Gerig, G. 2006. Framework for the statistical shape analysis of brain structures using SPHARM-PDM. Proceedings of the ISC/NA-MIC Workshop on Open Science at MICCAI 2006. *Insight Journal*, http://hdl.handle.net/1926/215.

Sutton, M.D., Briggs, D.E.G., Siveter, D.J., and Siveter, D.J. 2001. Methodologies for the Visualization and Reconstruction of Three-Dimensional Fossils from the Siluranian Herefordshire Lagerstätte. *Palaeontologia Electronica,* 4.1.2: 17 pp., 1MB. http://palaeo-electronica.org/2001_1/s2/issue1_01.htm

Szalay, F.S. 1977. Phylogenetic relationships and a classification of the eutherian Mammalia. In Hecht, M.K., Goody, P.C., and Hecht, B.M. (eds.), Major Patterns in Vertebrate Evolution, pp. 315-374.. Plenum Press: New York.

Szalay, F.S. 1994. Evolutionary History of the Marsupials and an Analysis of Osteological Characters. Cambridge: Cambridge University Press.

Taylor, M.E. 1970. Locomotion in some East African viverrids. *Journal of Mammalogy*, 51:42-51.

Taylor, M.E. 1976. The functional anatomy of the hindlimb of some African Viverridae (Carnivora). *Journal of Morphology*, 148:227-254.

Taylor, M.E. 1988. Foot structure and phylogeny in the Viverridae (Carnivora). Journal of Zoology London, 216:131-139.

Taylor, M.E. 1989. Locomotor adaptations. In Gittleman, J.L. (ed.), Carnivore Behavior, Ecology, and Evolution, pp. 382-409. Ithaca: Cornell University Press.

Turner, A. 1997. *The Big Cats and Their Fossil Relatives*. Columbia University Press, New York.

Ungar, P., and Williamson, M. 2000. Exploring the Effects of Toothwear on Functional Morphology: A Preliminary Study Using Dental Topographic Analysis. *Palaeontologia Electronica,* 3.1.1: 17 pp., 752KB. http://palaeo-electronica.org/2000_1/gorilla/issue1_00.htm

Van Valkenburgh, B. 1985. Locomotor diversity within past and present guilds of large predatory mammals. *Journal of Vertebrate Paleontology*, 11:406-428.

Werdelin, L. 1988. Studies of fossil hyaenids - the genera *Ictitherium* Roth and Wagner and *Sinictitherium* Kretzoi and a new species of *Ictitherium*. *Zoological Journal of the Linnean Society,* 93:93-105.

Wiley, D., Amenta, N., Alcantara, D., Ghosh, D., Kil, Y.J., Delson, E., Harcourt-Smith, W., St. John, K., Rohlf, F.J., and Hamann, B. 2005. Evolutionary morphing. *Proceedings, IEEE Visualization Conference*, 2005:431-438.

Wilhite, R. 2003. Digitizing Large Fossil Skeletal Elements for Three-Dimensional Applications. *Palaeontologia Electronica,* 5.2.4: 10 pp., 619KB. http://www-odp.tamu.edu/paleo/2002_2/scan/issue2_02.htm

Zelditch, M.L., Swiderski, D.L., Sheets, H.D., and Fink, W.L. 2004. *Geometric Morphometrics for Biologists*. Elsevier, Academic Press.